

Using machine learning to compress the matter transfer function $T(k)$

J. Bayron Orjuela-Quintana,^{1,2,*} Savvas Nesseris,^{2,†} and Wilmar Cardona^{3,‡}

¹*Departamento de Física, Universidad del Valle,*

Ciudad Universitaria Meléndez, Santiago de Cali 760032, Colombia

²*Instituto de Física Teórica UAM-CSIC, Universidad Autónoma de Madrid, Cantoblanco, 28049 Madrid, Spain*

³*ICTP South American Institute for Fundamental Research & Instituto de Física Teórica,
Universidade Estadual Paulista, 01140-070, São Paulo, Brazil*

The linear matter power spectrum $P(k, z)$ connects theory with large scale structure observations in cosmology. Its scale dependence is entirely encoded in the matter transfer function $T(k)$, which can be computed numerically by Boltzmann solvers, and can also be computed semi-analytically by using fitting functions such as the well-known Bardeen-Bond-Kaiser-Szalay (BBKS) and Eisenstein-Hu (EH) formulae. However, both the BBKS and EH formulae have some significant drawbacks. On the one hand, although BBKS is a simple expression, it is only accurate up to 10%, which is well above the 1% precision goal of forthcoming surveys. On the other hand, while EH is as accurate as required by upcoming experiments, it is a rather long and complicated expression. Here, we use the Genetic Algorithms (GAs), a particular machine learning technique, to derive simple and accurate fitting formulae for the transfer function $T(k)$. When the effects of massive neutrinos are also considered, our expression slightly improves over the EH formula, while being notably shorter in comparison.

I. INTRODUCTION

Almost two decades ago, the Λ CDM model was designated as the standard model of cosmology [1]. The concordance model is supported by several observations including the angular power spectrum of the cosmic microwave background [2], the distribution of galaxies at large scales [3–5], the late-time accelerated expansion of the Universe [6–8], the acoustic peaks as a fingerprint of the baryon acoustic oscillations in the early Universe [9–11]. These are just some of the many observational tests the Λ CDM model has overcome [12–16].

However, it is fair to mention that there exist some discrepancies in Λ CDM, such as the H_0 and σ_8 tensions [17, 18]. In general, alleviation of any of these tensions and others (see Refs. [18–23]) requires either the introduction of non-standard matter fields [24–26], or modifications to gravity [27–29]. Nonetheless, these theoretical alternatives, although physically viable in light of observations, usually introduce additional parameters, and hence they are not preferred over Λ CDM which is described by only six-parameters and provides an excellent fit to most of available data. In summary, Λ CDM is the simplest and most accurate model we currently have, given that no extensions to this paradigm have been detected so far [30–34].

One of the most important cosmological probes we have in favor of the concordance model is the distribution of galaxies at large scales [35, 36]. In order to

contrast our theoretical predictions against these observational data, it is necessary to extract the statistical information in the distribution of the large scale structure by computing the matter power spectrum, $P(k, z)$, which depends on the scale k and the redshift z . It can be shown that at first order in cosmological perturbations, and neglecting neutrinos, the dependence of $P(k, z)$ on k is encoded in the so-called matter transfer function $T(k)$, while the dependence on z is encoded in the growth factor $D_+(z)$ [37]. Therefore, for a fixed redshift, the matter power spectrum is a function only of the scale and its form is mostly described by the matter transfer function (see Sec. II).

The calculation of $P(k, z)$ generally requires to solve the multi-species Boltzmann equations, which can be done numerically in a matter of seconds using Boltzmann solvers, like the codes CLASS [38] and CAMB [39]. However, to have an accurate analytical description for specific quantities is always desirable. Following this line of thought, Bardeen, Bond, Kaiser, and Szalay found a fitting function for the transfer function considering radiation, baryons, and cold dark matter [40]. This BBKS formula is accurate up to 10% which is well below the precision of current data [41]. A better alternative is the fitting formula given by Eisenstein and Hu (EH) in Ref. [42]. The EH formula achieves a precision of around 1-2%, however it is given in terms of around 30 different, complicated expressions. These fitting formulae have been extensively used in the literature [43–45].

Machine learning has long been exploited in physics (see Ref. [46] for a review). In particular, machine learning has been used to address symbolic regression problems, i.e., finding an analytical expression that accurately describe a given data set [47–52]. In this work,

* john.orjuela@correounivalle.edu.co

† savvas.nesseris@csic.es

‡ wilmar.cardona@unesp.br

we use a specific machine learning technique known as Genetic Algorithms (GAs). GAs are loosely based on biological evolution concepts. In a nutshell, they attempt to improve the goodness of fit of the candidate expressions by randomly combining them and/or modifying some parts of them [53]. This approach seems to be suitable for finding analytical formulae for quantities of interest in cosmology [54–60]. Here, we use GAs to find analytical functions for the matter transfer function with accuracy of around 1% while being significantly shorter and thus easier to handle than other available formulae.

The organization of this paper is as follows. In Sec. III, we discuss existing fitting functions for the matter transfer function, while some generalities on the GA are given in Sec. IV. Then, we present our results in Sec. V, and in Sec. VI we summarize our conclusions.

II. THE MATTER TRANSFER FUNCTION

As mentioned in Sec. I, on large scales where nonlinearities are negligible, the linear matter power spectrum can be compared against observations of galaxy clustering, and gravitational lensing, among others [61–63]. In the concordance model, the primordial curvature perturbations generated during inflation are related to the gravitational potential at late times by means of two functions: *i*) the matter transfer function $T(k)$ which encodes its scale dependence and describes the evolution of perturbations during horizon crossing and transition from radiation to matter domination, *ii*) the growth factor $D_+(a)$ which describes the time-dependent growth of matter density perturbations at late times. Thus, the gravitational potential can be written as

$$\Phi(k, a) \propto \mathcal{R}(k)T(k)D_+(a), \quad (1)$$

where \mathcal{R} is the primordial curvature perturbation, and a is the scale factor. At late times, for sub-horizon modes, and neglecting massive neutrinos, this gravitational potential can be related to the matter contrast δ_m by means of the Poisson equation:

$$k^2\Phi(k, a) \propto \rho_m a^2 \delta_m(k, a), \quad (2)$$

where ρ_m is the background density of pressure-less matter. Taking into account that the primordial perturbations are nearly Gaussian with zero mean [14], the linear matter power spectrum can be written as [37]

$$P(k, a) \propto \frac{k^{n_s}}{\Omega_m^2} D_+^2(a) T^2(k), \quad (3)$$

where n_s is the scalar spectral index of primordial fluctuations, and Ω_m is the density parameter of pressure-less matter. Therefore, for a fixed redshift, the power

spectrum is given by

$$P(k) \propto k^{n_s} T^2(k), \quad (4)$$

namely, it is fully determined by the transfer function. In this work, we present a very accurate fitting formula for $T(k)$ as a function of the density of baryons and matter, such that it is straightforward to compute the linear matter power spectrum.

As it is well-known from experiments, neutrinos are massive [64, 65]. At sufficiently small scales, free streaming massive neutrinos imprint their effects on the cosmological evolution, which translates to a further suppression of the matter power spectrum. In this case, the growth factor acquires a scale dependency, making non-trivial a similar separation as in Eq. (3). However, for a fixed redshift, it is possible to absorb all the scale dependent effects in an effective matter transfer function, as shown in Ref. [66].

III. PREVIOUS FITTING FORMULAE

Before the advent of fast and accurate Boltzmann solvers, several attempts were made to describe analytically the matter transfer function. One of the most remarkable results of this pursuit is the BBKS formula which is based on previous fitting formulae by Bardeen, Bond, Efstathiou, and Szalay [67–69]. In the case that $\Omega_b \ll \Omega_m$, that is, the main contribution to the matter content is in the form of Cold Dark Matter (CDM), the BBKS formula reads

$$T_{c,\text{BBKS}}(k) \equiv \frac{\ln(1 + 2.34q)}{2.34q} \left[1 + 3.89q + (16.1q)^2 + (5.46q)^3 + (6.71q)^4 \right]^{-1/4}, \quad (5)$$

where

$$q(k) \equiv \frac{k\theta^{1/2}}{(\omega_m - \omega_b)\text{Mpc}^{-1}}, \quad \theta \equiv \frac{\rho_r}{1.68\rho_\gamma}, \quad (6)$$

and $\omega_X \equiv \Omega_X h^2$ the reduced density parameter (Ω_X being the density parameter of species X), h the reduced Hubble constant, ρ_X the background density, and $X = b, c, m, r, \nu, \gamma$ denotes baryons, CDM, pressure-less matter, radiation, neutrinos, photons, respectively. When ω_b is not negligible, the transfer function is modified as

$$T_{\text{BBKS}}(k; \omega_b, \omega_m) \equiv T_{c,\text{BBKS}}(k) \left[1 + \frac{(kR_{\text{Jr}})^2}{2} \right]^{-1}, \quad (7)$$

where $R_{\text{Jr}} \equiv 1.6(\omega_m - \omega_b)^{-1/2}$ kpc.

A more accurate formula was presented by Eisenstein and Hu in Ref. [42]. This formula is constructed from several physically motivated terms, such as acoustic oscillations, Compton drag, velocity overshoot, baryon infall, adiabatic damping, Silk damping, CDM suppression. These terms accurately describe, for instance, the suppression in the transfer function on small scales due to the presence of baryons, and the amplitude and location of baryonic oscillations [42]. All the mentioned effects are taken into account in the EH formula by around 30 expressions, which we present in Appendix A.

The free-streaming scale of massive neutrinos is imprinted in the transfer function, which translates to a further suppression on the smallest scales. In Ref. [66], Eisenstein and Hu provided a fitting formula when baryons, CDM and massive neutrinos are considered. The latter formulation also requires around 30 expressions, which we write in Appendix B.

Although accurate and based on known physics, the EH expressions are, at the end, fitting formulae and not a fundamental result. As we will show, our GA fitting formulae are notably shorter, as accurate as the EH expression when only baryons and CDM are considered, and slightly more accurate when the effects of massive neutrinos are non-negligible. Therefore, our GA provides compelling alternatives to other available fitting formulae.

IV. GENETIC ALGORITHMS

Here we briefly review the GA, which can be used as a stochastic symbolic regression approach. Basically, the symbolic regression problem consists in finding a fitting function for a given dataset, and thus defining a non-parametric approach to describe data. There are several free and commercial codes to perform symbolic regression [47–52]. The GAs have been widely used in several branches of physics, like particle physics [70–72], astrophysics [73, 74], and cosmology [75–80].

In the GA, which is a machine learning technique inspired by concepts in evolutionary biology [53], a population composed by several individuals (mathematical expressions in this case) evolves expecting to optimize the goodness of fit of next generations to a given dataset, which can be measured by a goodness of fit function, usually taken to be a χ^2 . Each individual is in turn composed by a selected set of basic operations, i.e., the grammar, which are randomly selected depending on the “nucleotides”. These nucleotides are random numbers which in group form the genes setting the mathematical expression of an individual. Once the initial population is created, i.e., the progenitors, the goodness of fit of each individual is measured and, using a tournament scheme, a set containing the best prospects

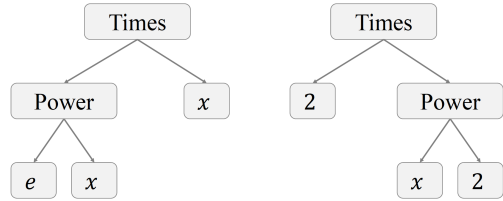


FIG. 1. Two exemplifying grammatical expressions corresponding to the individuals xe^x and $2x^2$.

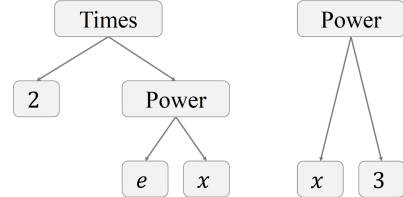


FIG. 2. The two selected individuals have been combined to produce two new individuals: $2e^x$ and x^3 .

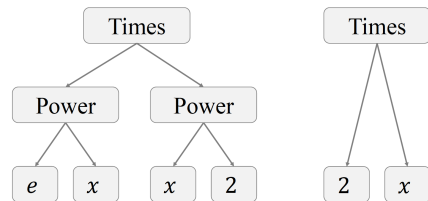


FIG. 3. The two selected individuals have suffered a mutation to become two new individuals: x^2e^x and $2x$.

is selected for reproduction and survival to contribute to the next generation.

The reproduction is carried out by the so-called genetic operators, namely, crossover and mutation. In the crossover stage, two individuals are randomly combined to produce new individuals sharing characteristics of both parents. In the mutation stage, one nucleotide of an individual is randomly selected and modified. This process is repeated for a given number of generations.

Now, we describe the way reproduction works in GA with an example. In Fig. 1, there are two expressions in tree representation, i.e., two individuals xe^x and $2x^2$. Let us assume that these individuals were selected for reproduction. Figure 2 shows possible combinations of the two individuals, while Fig. 3 shows their possible mutations. For instance, the new individual in the left-hand side of Fig. 2 is born from the combination of the expressions e^x and 2 from its parents, while the other individual is made from the remaining parts, x and x^2 , using the proper basic operation “Times” or product. During the mutation stage, a selected individual is altered randomly. As shown in Fig. 3, for instance, the

	Expression	% Accuracy
BBKS	Eq. (7)	8.70957
EH	Appendix A	0.777504
GA	Eq. (11)	0.815012

TABLE I. Expression and accuracy of the fitting formulae for the matter transfer function as a function of k , ω_b , and ω_m . Although the GA does not provide a more accurate formula than the EH formula, the simplicity of the former [Eq. (11)] is a major improvement over the EH formula (Appendix A).

individual xe^x mutated to x^2e^x , and the individual $2x^2$ mutated to $2x$.

V. RESULTS

In this section, we present our fitting formulae for the matter transfer function. We firstly consider the case when $T(k)$ depends only on the amount of baryons and matter, and then we add the effects of massive neutrinos. For both cases, we start describing how the data for the fitting process was gathered using CLASS, and later we proceed to introduce the simple fitting function we found using the GA.

A. Baryons and Matter

1. Data

We use the Boltzmann solver CLASS to compute the linear matter transfer function¹ $T(k)$. In this code, each pair of parameters $\{\omega_b, \omega_m\}$ defines a cosmology for which we can compute the gravitational potential Φ as a function of the scale k at a fixed redshift. Hence, to see the dependence of the transfer function on these parameters, we make a grid of 4×4 pairs of $\{\omega_b, \omega_m\}$ and compute the gravitational potential for each pair. We consider that $\omega_b \in [0.0214, 0.0234]$, and $\omega_m \in [0.13, 0.15]$, which are around 10σ from the best-fit values found by the Planck Collaboration [2]. For each considered cosmology (16 in total), CLASS retrieves 114 points $\{k, \Phi\}$. Therefore, our preliminary dataset is composed by 1824 points whose rows are given as $\{k, \omega_b, \omega_m, \Phi\}$. Now, since the transfer function is basically the normalized potential, we normalize each of the 16 sub-datasets to

get $T(k; \omega_b, \omega_m)$. At the end, our final dataset is a table of dimensions 1824×4 with data points given as $\{k, \omega_b, \omega_m, T\}$.

We quantify the goodness of fit of a given analytical expression by the following function

$$\% \text{Acc} = \frac{100}{N} \sum_{i=1}^N \left| \frac{T_{i, \text{CLASS}} - T_{i, \text{analytical}}}{T_{i, \text{CLASS}}} \right|, \quad (8)$$

where $N = 1824$ is the number of data points in our dataset, and T_i is a simplified notation for the transfer function evaluated at k_i , ω_{b_i} , and ω_{m_i} .

2. Fitting Formula from the GA

Here, we give a few details concerning the specific GA configuration we used and present our fitting formula.

As explained in Sec. IV, the GA looks for a fitting formula to a dataset by evolving the population, which is composed by expressions combining specific operations (grammar) and coefficients. Schematically, our GA is searching for a function of the form

$$T_{\text{GA}}(x) \equiv [1 + f_{\text{GA}}(x)]^{-1/4}, \quad (9)$$

where

$$x \equiv \frac{k \text{ Mpc}}{\omega_m - \omega_b}, \quad f_{\text{GA}} \equiv \sum_{i=1}^4 a_i g_i ((b_i x)^{c_i}). \quad (10)$$

We see that x is a dimensionless quantity since k is given in units $[h \text{ Mpc}^{-1}]$, h the reduced Hubble parameter. The constants a_i , b_i , c_i are non-negative random numbers, and g_i is an operation in the grammar set, which we consider to be simply of the form $\{x\}$. The quantities a_i , g_i , b_i , and c_i are the 4 nucleotides. The sum goes from 1 to 4 because we are considering that the genome of the individuals is formed by 4 genes, each one composed by the 4 nucleotides, such that the chromosomes are 4×4 matrices.

It should be noted that the number of genes has to be fixed before the code starts running and we have chosen the number four for two reasons: i) first, from experience we have found that a number of four genes is a compromise (found by trial and error) on the length of the function, as less than is not enough to fit the data, while a much larger number slows down the code considerably, ii) second, if the number of genes is too high, then this could obviously lead to overfitting or instabilities in the fitting. Furthermore, even though at first sight it seems so, the parameters a_i and b_i , in general are not degenerate as b_i appears inside the grammar function, however there may be some degeneracies only when the grammar is linear.

¹ Note that CLASS can take into account non-linear effects via fitting functions such as HALOFIT [81]. Here however we focus on the linear regime and neglect non-linear contributions when generating the data.

Overall, this configuration, although restrictive, fixes the length of the expressions, thus avoiding over-fitting problems. A couple of reasons motivate the specific forms of Eqs. (9) and (10): *i*) the transfer function has specific limits: $T \rightarrow 0$ when $k \rightarrow \infty$, and $T \rightarrow 1$

when $k \rightarrow 0$, *ii*) the transfer function only takes on non-negative values, and *iii*) $T(k)$ is smooth.

Now, we present our fitting formula when only baryons and matter are considered. Using the configuration of the GA as explained, the stochastic search ended up with the function

$$T_{\text{GA}}(k; \omega_b, \omega_m) = [1 + 59.0998 x^{1.49177} + 4658.01 x^{4.02755} + 3170.79 x^{6.06} + 150.089 x^{7.28478}]^{-1/4}, \quad (11)$$

whose goodness of fit, as measured by Eq. (8), is $\% \text{Acc}_{\text{GA}} = 0.815012$. The accuracy of the BBKS formula in Eq. (7) is $\% \text{Acc}_{\text{BBKS}} = 8.70957$, and for the EH formula is $\% \text{Acc}_{\text{EH}} = 0.777504$. We compile these results in Table I. In Fig. 4, we compare the performance of the fitting formulae. As it can be seen in the left panel of this figure, the three formulae are very accurate on the large scales ($k < 0.01 h \text{ Mpc}^{-1}$), while for smaller scales ($k > 0.01 h \text{ Mpc}^{-1}$), where the effects of baryons are most prominent on the cosmological evolution, the accuracy of the three formulae decrease. However, we note that our GA formula and the EH formula can be accurate up to 5%, while the BBKS formula is accurate up to 18% in these scales. We would like to emphasize that our GA formula in Eq. (11) is remarkably simpler than the EH formula which is described by around 30 expressions which occupy the whole Appendix A, while their difference in accumulative accuracy is just about 0.04. We also want to stress that, in principle, the GA could get even better results if some modifications are introduced. For instance, a larger grammar set and a more complex f_{GA} function [instead of Eq. (10)]. Nonetheless, our choices avoid over-fitting while yielding a smooth transfer function with the correct limits in k .

B. Baryons, Matter and Massive Neutrinos

1. Data

Apart of baryons and cold dark matter, massive neutrinos can contribute to the matter content once they are freely streaming. We can take into account the effects of massive neutrinos in the matter transfer function using CLASS. We compute $T(k)$ at redshift zero

as a function of ω_b, ω_m in the same ranges as in Sec. V A, and $\omega_\nu \equiv 0.0107(\sum_\nu m_\nu / 1.0 \text{ eV})$, assuming just one massive neutrino, and that the total mass of massive neutrinos is in the range $0.06 \text{ eV} \leq \sum m_\nu \leq 0.12 \text{ eV}$. The lower bound of the later constraint corresponds to the minimum mass allowed from neutrino flavour oscillation experiments [64], and the upper bound is the maximum mass value allowed by Planck [2]. In this case, we get a grid of $4 \times 4 \times 4$ data points for $\{\omega_b, \omega_m, \omega_\nu\}$ and compute the gravitational potential for each triad. Again, for each considered cosmology (64 in total), CLASS retrieves 114 points $\{k, \Phi\}$. Normalizing the potential to get the transfer function, our final data set is a table of dimensions 7296×5 with data points given as $\{k, \omega_b, \omega_m, \omega_\nu, T\}$. We use Eq. (8) to quantify the goodness of fit of the analytical expressions, but now $N = 7296$ is the number of data points in our dataset, and T_i is the transfer function evaluated at $k_i, \omega_{b_i}, \omega_{m_i}$, and ω_{ν_i} .

2. Fitting Formula from the GA

Based on the success of the GA in finding an accurate formula for $T(k)$ when neutrinos are massless, this time our GA is looking for a function of the form

$$T_{\text{GA}}(y) \equiv [1 + f_{\text{GA}}(y)]^{-1/4}, \quad (12)$$

where

$$y \equiv \frac{k \text{ Mpc}}{\omega_m - \omega_b + \omega_\nu}, \quad f_{\text{GA}} \equiv \sum_{i=1}^4 a_i g_i ((b_i y)^{c_i}). \quad (13)$$

Now, we present our fitting formula which considers baryons, matter, and one massive neutrino:

$$T_{\text{GA}}(k; \omega_b, \omega_m) = [1 + 56.4933 y^{1.48261} + 3559.23 y^{3.76407} + 4982.44 y^{5.68246} + 374.167 y^{7.14558}]^{-1/4}, \quad (14)$$

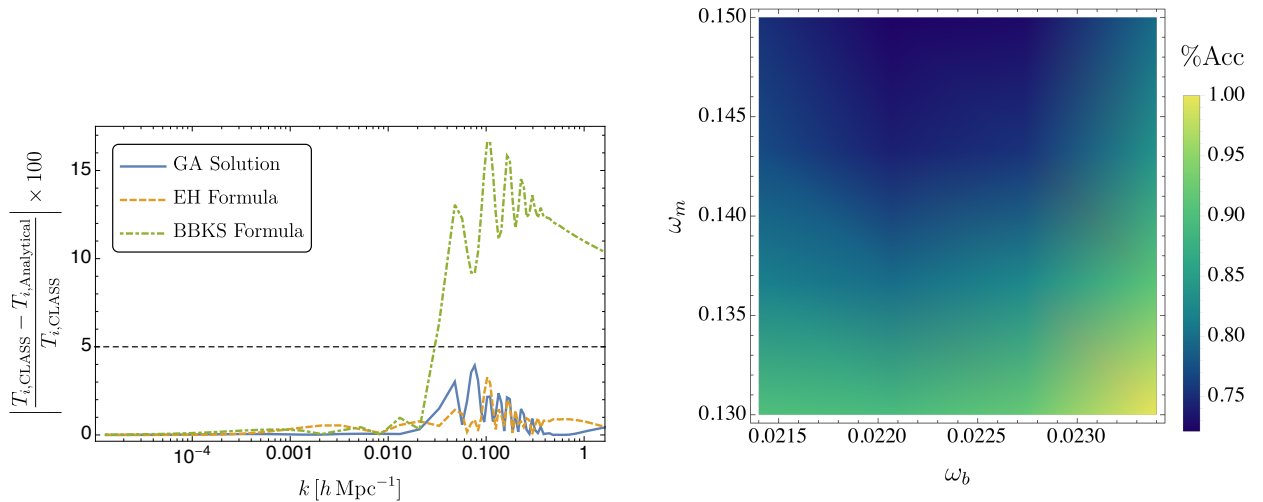


FIG. 4. (Left) Accuracy of the BBKS (green dot-dashed line), EH (mustard dashed line), and the GA (blue solid line) fitting formulae as a function of the scale k and fixed $\{\omega_m, \omega_b\}$. The parameters for these plots are: $\omega_b = 0.02273$, and $\omega_m = 0.1366$. Note that the accuracy of the three formulae notably decrease on the scales where the effects of baryons are most prominent on the cosmological evolution. However, the accuracy of the EH and GA formulae are below 5% in this scale. (Right) Average accuracy of the GA fitting formula for all k as a function of $\{\omega_m, \omega_b\}$. As it can be seen, the formula is up to 1% accurate in overall.

	Expression	% Accuracy
EH	Appendix B	1.23449
GA	Eq. (14)	0.993916

TABLE II. Expression and accuracy of the fitting formulae for the matter transfer function as a function of k , ω_b , ω_m , and ω_ν . Although the accuracy of both formulations are similar, the simplicity of the GA function in Eq. (14) is a major improvement over the EH formula, which is fully displayed in Appendix B.

whose goodness of fit, as measured by Eq. (8), is $\%Acc_{GA} = 0.993916$. The accuracy of the extended EH formula considering massive neutrinos is $\%Acc_{EH} = 1.23449$. We compile these results in Table II. In Fig. 5, we compare the performance of the fitting formulae. Similar to the last section, the formulae are more accurate on large scales ($k < 0.01 h \text{ Mpc}^{-1}$) than on the smaller scales ($k > 0.01 h \text{ Mpc}^{-1}$). Note in the left panel of this figure that the accuracy of the GA formula is below the 5% in the whole range of k . Furthermore, the GA formula (14) is significantly simpler than the EH formula, whose description requires around 30 expression which we give in full in Appendix B. Our result is a compelling analytical alternative to compute the matter transfer function.

VI. CONCLUSIONS

Genetic Algorithms (GAs), a machine learning technique, have been previously used to obtain improved formulation of cosmological quantities of interest such as the redshift at recombination and the sound horizon at drag epoch [58], and also to perform consistency tests to probe for deviations from Λ CDM [32, 55, 56, 59, 60, 82, 83]. Here we used the GA to find analytical alternatives to existing fitting functions for the matter transfer function, such as the BBKS and the EH formulae.

When the transfer function depends only on ω_b and ω_m , the GA finds a very simple fitting formula for $T(k)$ [see Eq. (11)], which is as accurate as the EH formula, while being significantly shorter (see Appendix A). In a more realistic scenario, at least one neutrino should be massive. In this case, our GA finds a fitting function which is both more accurate and notably simpler [see Eq. (14)] than the EH formula in Appendix B. The simplicity of the GA fitting formulae and their accuracy represent a major improvement over other existing analytical formulations of the matter transfer function which are extensively used in the literature [43–45]. Therefore, the GA formulae in Eqs. (11) and (14) are compelling semi-analytic alternatives to easily and accurately compute the matter power spectrum.

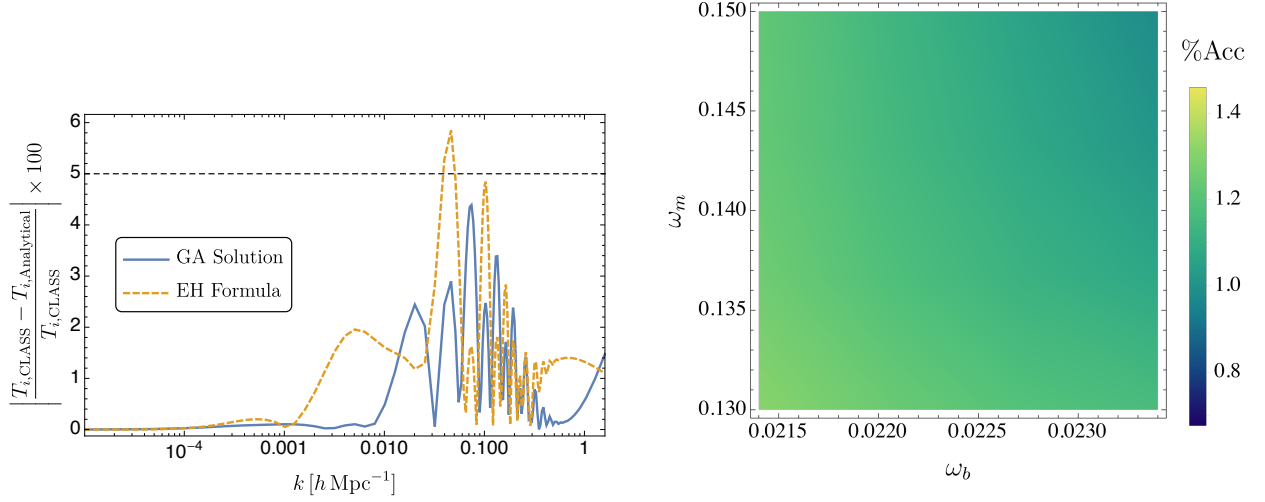


FIG. 5. (Left) Accuracy of the EH (mustard dashed line), and the GA (blue solid line) fitting formulae as a function of the scale k for fixed $\{\omega_m, \omega_b, \omega_\nu\}$. The parameters for these plots are: $\omega_b = 0.02206$, $\omega_m = 0.1499$, and $\omega_\nu = 0.0008599$ which corresponds to a mass of $\sum_\nu m_\nu = 0.08$ eV. As can be seen, the accuracy of the GA formula is below 5% on the whole range of k considered here. (Right) Average accuracy of the GA fitting formula for all k and ω_ν as a function of $\{\omega_m, \omega_b\}$. As it can be seen, the formula is around 1% accurate in overall.

ACKNOWLEDGEMENTS

The authors would like to thank R. Arjona for useful discussions at a very early stage of this project, and also to Jose Palacios for carefully reading the manuscript and providing useful comments. BOQ would like to express his gratitude to the Instituto de Física Teórica UAM-CSIC, in Universidad Autónoma de Madrid, for the hospitality and kind support during all the stages of this work. BOQ is also supported by Patrimonio Autónomo - Fondo Nacional de Financiamiento para la Ciencia, la Tecnología y la Innovación Francisco José de Caldas (MINCIENCIAS - COLOMBIA) Grant No. 110685269447 RC-80740-465-2020, projects 69723 and 69553. WC acknowledges financial support from the São Paulo Research Foundation (FAPESP) through grant #2021/10290-2. This research was supported by resources supplied by the Center for Scientific Computing (NCC/GridUNESP) of the São Paulo State University (UNESP). SN acknowledges support from the research projects PGC2018-094773-B-C32 and PID2021-123012NB-C43, and by the Spanish Research Agency (Agencia Estatal de Investigación) through the Grant IFT Centro de Excelencia Severo Ochoa No CEX2020-001007-S, funded by MCIN/AEI/10.13039/501100011033.

NUMERICAL CODES

The genetic algorithm code used here can be found in the GitHub repository <https://github.com/BayronO/Transfer-Function-GA> of BOQ. This code is based on the GA code by SN which can be found at <https://github.com/snesseris/Genetic-Algorithms>.

Appendix A: EH Formula

The transfer function given by Eisenstein and Hu [42] has the following form:

$$T(k) = \frac{\Omega_b}{\Omega_0} T_b(k) + \frac{\Omega_c}{\Omega_0} T_c(k), \quad (\text{A1})$$

where $\Omega_0 = \Omega_b + \Omega_c$. The terms involved in this formula are the following:

$$T_b = \left[\frac{\tilde{T}_0(k; 1, 1)}{1 + (ks/5.2)^2} + \frac{\alpha_b}{1 + (\beta_b/ks)^3} e^{-\left(\frac{k}{k_{\text{Siik}}}\right)^{1.4}} \right] j_0(k\tilde{s}), \quad (\text{A2})$$

$$T_c = f\tilde{T}_0(k, 1, \beta_c) + (1 - f)\tilde{T}_0(k, \alpha_c, \beta_c), \quad (\text{A3})$$

$$\tilde{T}_0(k, \alpha_c, \beta_c) = \frac{\ln(e + 1.8\beta_c q)}{\ln(e + 1.8\beta_c q) + Cq^2}, \quad (\text{A4})$$

$$f = \frac{1}{1 + (ks/5.4)^4}, \quad (\text{A5})$$

$$C = \frac{14.2}{\alpha_c} + \frac{386}{1 + 69.9q^{1.08}}, \quad (\text{A6})$$

$$q = \frac{k}{13.41k_{\text{eq}}}, \quad (\text{A7})$$

$$R \equiv 3\rho_b/4\rho_\gamma = 31.5\omega_b\Theta_{2.7}^{-4}(z/10^3)^{-1}, \quad (\text{A8})$$

$$k_{\text{Silk}} = 1.6\omega_b^{0.52}\omega_0^{0.73} \left[1 + (10.4\omega_0)^{-0.95} \right] \text{Mpc}^{-1}, \quad (\text{A9})$$

$$k_{\text{eq}} = 7.46 \times 10^{-2} \omega_0 \Theta_{2.7}^{-2} \text{Mpc}^{-1}, \quad (\text{A10})$$

$$\alpha_b = 2.07k_{\text{eq}}s(1 + R_d)^{-3/4}G\left(\frac{1 + z_{\text{eq}}}{1 + z_d}\right), \quad (\text{A11})$$

$$\beta_b = 0.5 + \frac{\Omega_b}{\Omega_0} + \left(3 - 2\frac{\Omega_b}{\Omega_0}\right) \sqrt{(17.2\omega_0)^2 + 1}, \quad (\text{A12})$$

$$\beta_{\text{node}} = 8.41\omega_0^{0.435}, \quad (\text{A13})$$

$$s = \frac{2}{3k_{\text{eq}}} \sqrt{\frac{6}{R_{\text{eq}}}} \ln \frac{\sqrt{1 + R_d} + \sqrt{R_d + R_{\text{eq}}}}{1 + \sqrt{R_{\text{eq}}}}, \quad (\text{A14})$$

$$\tilde{s} = s \left[1 + \left(\frac{\beta_{\text{node}}}{ks} \right)^3 \right]^{-1/3}, \quad (\text{A15})$$

$$G(y) = -6y\sqrt{1 + y} + y(2 + 3y) \ln \left(\frac{\sqrt{1 + y} + 1}{\sqrt{1 + y} - 1} \right), \quad (\text{A16})$$

$$y \equiv \frac{1 + z_{\text{eq}}}{1 + z}, \quad (\text{A17})$$

$$\alpha_c = a_1^{-\Omega_b/\Omega_0} a_2^{-(\Omega_b/\Omega_0)^3}, \quad (\text{A18})$$

$$a_1 = (46.9\omega_0)^{0.670} [1 + (32.1\omega_0)^{-0.532}], \quad (\text{A19})$$

$$a_2 = (12.0\omega_0)^{0.424} [1 + (45.0\omega_0)^{-0.582}], \quad (\text{A20})$$

$$\beta_c^{-1} = 1 + b_1[(\Omega_c/\Omega_0)^{b_2} - 1], \quad (\text{A21})$$

$$b_1 = 0.944[1 + (458\omega_0)^{-0.708}]^{-1}, \quad (\text{A22})$$

$$b_2 = (0.395\omega_0)^{-0.0266}. \quad (\text{A23})$$

$$z_{\text{eq}} = 2.50 \times 10^4 \omega_0 \Theta_{2.7}^{-4}, \quad (\text{A24})$$

$$z_d = 1291 \frac{\omega_0^{0.251}}{1 + 0.659\omega_0^{0.828}} \left[1 + b_{1,z}\omega_b^{b_{2,z}} \right], \quad (\text{A25})$$

$$b_{1,z} = 0.313\omega_0^{-0.419} [1 + 0.607\omega_0^{0.674}], \quad (\text{A26})$$

$$b_{2,z} = 0.238\omega_0^{0.223}, \quad (\text{A27})$$

where we have defined $\omega_0 = (\Omega_c + \Omega_b)h^2$, and $T_{\text{CMB}} \equiv 2.7\Theta_{2.7} \text{K}$, $R_d \equiv R(z_d)$ and $R_{\text{eq}} \equiv R(z_{\text{eq}})$

Appendix B: EH Formula with Massive Neutrinos

The transfer function given by Eisenstein and Hu considering massive neutrinos has the following form [66]:

$$T_{cb\nu}(k, z) = T_{\text{master}}(k) \frac{D_{cb\nu}(k, z)}{D_1(z)}, \quad (\text{B1})$$

The terms involved in this formula are the following:

$$T_{\text{master}}(k) = T_{\text{sup}}(k)B(k), \quad (\text{B2})$$

$$D_{cb\nu}(z, q) = \left[f_{cb}^{0.7/p_{cb}} + \left(\frac{D_1(z)}{1 + y_{\text{fs}}(q; f_\nu)} \right)^{0.7} \right]^{p_{cb}/0.7} \times D_1(z)^{1-p_{cb}}, \quad (\text{B3})$$

$$D_1(z) = \left(\frac{1 + z_{\text{eq}}}{1 + z} \right) \frac{5\Omega(z)}{2} \left\{ \Omega(z)^{4/7} - \Omega_\Lambda(z) + \left[1 + \frac{\Omega(z)}{2} \right] \left[1 + \frac{\Omega_\Lambda(z)}{70} \right] \right\}^{-1}, \quad (\text{B4})$$

$$\Omega(z) = \Omega_0(1 + z)^3 g^{-2}(z), \quad (\text{B5})$$

$$\Omega_\Lambda(z) = \Omega_\Lambda g^{-2}(z), \quad (\text{B6})$$

$$g^2(z) = (1 - \Omega_0 - \Omega_\Lambda)(1 + z)^2 + \Omega_0(1 + z)^3 + \Omega_\Lambda, \quad (\text{B7})$$

$$T_{\text{sup}}(k) = \frac{L}{L + Cq_{\text{eff}}^2}, \quad (\text{B8})$$

$$L = \ln(e + 1.84\beta_c \sqrt{\alpha_\nu} q_{\text{eff}}), \quad (\text{B9})$$

$$C = 14.4 + \frac{325}{1 + 60.5q_{\text{eff}}^{1.08}}, \quad (\text{B10})$$

$$\beta_c = (1 - 0.949f_{\nu b})^{-1}, \quad (\text{B11})$$

$$y_{\text{fs}}(q) = 17.2f_\nu(1 + 0.488f_\nu^{-7/6})(qN_\nu/f_\nu)^2, \quad (\text{B12})$$

$$q = \frac{k}{\text{Mpc}^{-1}} \Theta_{2.7}^2 \omega_0^{-1}, \quad (\text{B13})$$

$$B(k) = 1 + \frac{1.24f_\nu^{0.64}N_\nu^{0.3+0.6f_\nu}}{q_\nu^{-1.6} + q_\nu^{0.8}}, \quad (\text{B14})$$

$$q_\nu = 3.92q \sqrt{\frac{N_\nu}{f_\nu}} \quad (\text{B15})$$

$$f_c = \frac{\Omega_b}{\Omega_m + \Omega_\nu}, \quad f_\nu = \frac{\Omega_\nu}{\Omega_m + \Omega_\nu},$$

$$f_{cb} = \frac{\Omega_m}{\Omega_m + \Omega_\nu}, \quad f_{\nu b} = \frac{\Omega_b + \Omega_\nu}{\Omega_m + \Omega_\nu}, \quad (\text{B16})$$

$$q_{\text{eff}} = \frac{k\Theta_{2.7}^2}{\Gamma_{\text{eff}} \text{Mpc}^{-1}}, \quad (\text{B17})$$

$$\Gamma_{\text{eff}} = \omega_0 \left[\sqrt{\alpha_\nu} + \frac{1 - \sqrt{\alpha_\nu}}{1 + (0.43ks)^4} \right], \quad (\text{B18})$$

$$\alpha_\nu = \frac{f_c}{f_{cb}} \frac{5 - 2(p_c + p_{cb})}{5 - 4p_{cb}} \quad (\text{B19})$$

$$\begin{aligned} & \times \frac{1 - 0.553f_{\nu b} + 0.126f_{\nu b}^3}{1 - 0.193\sqrt{f_\nu N_\nu} + 0.169f_\nu N_\nu^{0.2}} (1 + y_d)^{p_{cb} - p_c} \\ & \times \left[1 + \frac{p_c - p_{cb}}{2} \left(1 + \frac{1}{(3 - 4p_c)(7 - 4p_{cb})} \right) \right] \\ & \times (1 + y_d)^{-1}, \end{aligned} \quad (\text{B20})$$

$$p_c \equiv \frac{1}{4} \left[5 - \sqrt{1 + 24f_c} \right], \quad (\text{B21})$$

$$p_{cb} \equiv \frac{1}{4} \left[5 - \sqrt{1 + 24f_{cb}} \right], \quad (\text{B22})$$

$$z_{\text{eq}} = 2.50 \times 10^4 \omega_0 \Theta_{2.7}^{-4}, \quad (\text{B23})$$

$$z_d = 1291 \frac{\omega_0^{0.251}}{1 + 0.659\omega_0^{0.828}} \left[1 + b_{1,z} \omega_b^{b_{2,z}} \right], \quad (\text{B24})$$

$$b_1 = 0.313\omega_0^{-0.419} \left[1 + 0.607\omega_0^{0.674} \right], \quad (\text{B25})$$

$$b_2 = 0.238\omega_0^{0.223}, \quad (\text{B26})$$

$$y \equiv \frac{1 + z_{\text{eq}}}{1 + z}, \quad (\text{B27})$$

$$s = \frac{44.5 \ln(9.83\omega_0)}{\sqrt{1 + 10\omega_b^{3/4}}} \text{Mpc}, \quad (\text{B28})$$

where N_ν is the number of massive neutrinos, Ω_Λ is the density parameter of cosmological constant, and we have redefined some terms like $\Omega_0 = \Omega_c + \Omega_b + \Omega_\nu$, and $\omega_0 = \Omega_0 h^2$.

-
- [1] P. J. E. Peebles, *Cosmology's Century: An Inside History of Our Modern Understanding of the Universe*. Princeton University Press, 2020.
- [2] **Planck** Collaboration, N. Aghanim *et al.*, “Planck 2018 results. VI. Cosmological parameters,” *Astron. Astrophys.* **641** (2020) A6, [arXiv:1807.06209 \[astro-ph.CO\]](#). [Erratum: *Astron. Astrophys.* 652, C4 (2021)].
- [3] **DES** Collaboration, M. A. Troxel *et al.*, “Dark Energy Survey Year 1 results: Cosmological constraints from cosmic shear,” *Phys. Rev. D* **98** no. 4, (2018) 043528, [arXiv:1708.01538 \[astro-ph.CO\]](#).
- [4] **DES** Collaboration, T. M. C. Abbott *et al.*, “Dark Energy Survey Year 1 Results: Constraints on Extended Cosmological Models from Galaxy Clustering and Weak Lensing,” *Phys. Rev. D* **99** no. 12, (2019) 123505, [arXiv:1810.02499 \[astro-ph.CO\]](#).
- [5] **DES** Collaboration, T. M. C. Abbott *et al.*, “Dark Energy Survey Year 3 results: Cosmological constraints from galaxy clustering and weak lensing,” *Phys. Rev. D* **105** no. 2, (2022) 023520, [arXiv:2105.13549 \[astro-ph.CO\]](#).
- [6] **Supernova Search Team** Collaboration, A. G. Riess *et al.*, “Observational evidence from supernovae for an accelerating universe and a cosmological constant,” *Astron. J.* **116** (1998) 1009–1038, [arXiv:astro-ph/9805201](#).
- [7] **Supernova Cosmology Project** Collaboration, S. Perlmutter *et al.*, “Measurements of Ω and Λ from 42 high redshift supernovae,” *Astrophys. J.* **517** (1999) 565–586, [arXiv:astro-ph/9812133](#).
- [8] **Supernova Search Team** Collaboration, A. G. Riess *et al.*, “Type Ia supernova discoveries at $z > 1$ from the Hubble Space Telescope: Evidence for past deceleration and constraints on dark energy evolution,” *Astrophys. J.* **607** (2004) 665–687, [arXiv:astro-ph/0402512](#).
- [9] W. percival *et al.*, “Baryon acoustic oscillations in the Sloan Digital Sky Survey Data Release 7 galaxy sample,” *Monthly Notices of the Royal Astronomical Society* **401** no. 4, (2010) 2148–2168.
- [10] C. Blake *et al.*, “The WiggleZ Dark Energy Survey: mapping the distance-redshift relation with baryon

- acoustic oscillations,” *Monthly Notices of the Royal Astronomical Society* **418** no. 3, (2011) 1707–1724.
- [11] E. Aubourg *et al.*, “Cosmological implications of baryon acoustic oscillation measurements,” *Phys. Rev. D* **92** no. 12, (2015) 123516, [arXiv:1411.1074 \[astro-ph.CO\]](#).
- [12] **Boomerang** Collaboration, P. de Bernardis *et al.*, “A Flat universe from high resolution maps of the cosmic microwave background radiation,” *Nature* **404** (2000) 955–959, [arXiv:astro-ph/0004404](#).
- [13] A. H. Jaffe *et al.*, “Recent results from the maxima experiment,” *New Astron. Rev.* **47** (2003) 727–732, [arXiv:astro-ph/0306504](#).
- [14] **Planck** Collaboration, Y. Akrami *et al.*, “Planck 2018 results. X. Constraints on inflation,” *Astron. Astrophys.* **641** (2020) A10, [arXiv:1807.06211 \[astro-ph.CO\]](#).
- [15] **Planck** Collaboration, Y. Akrami *et al.*, “Planck 2018 results. VII. Isotropy and Statistics of the CMB,” *Astron. Astrophys.* **641** (2020) A7, [arXiv:1906.02552 \[astro-ph.CO\]](#).
- [16] **DES** Collaboration, T. M. C. Abbott *et al.*, “Cosmological Constraints from Multiple Probes in the Dark Energy Survey,” *Phys. Rev. Lett.* **122** no. 17, (2019) 171301, [arXiv:1811.02375 \[astro-ph.CO\]](#).
- [17] A. G. Riess *et al.*, “Large Magellanic Cloud Cepheid Standards Provide a 1% Foundation for the Determination of the Hubble Constant and Stronger Evidence for Physics beyond Λ CDM,” *Astrophys. J.* **876** no. 1, (2019) 85, [arXiv:1903.07603 \[astro-ph.CO\]](#).
- [18] E. Abdalla *et al.*, “Cosmology intertwined: A review of the particle physics, astrophysics, and cosmology associated with the cosmological tensions and anomalies,” *JHEAp* **34** (2022) 49–211, [arXiv:2203.06142 \[astro-ph.CO\]](#).
- [19] A. Joyce, L. Lombriser, and F. Schmidt, “Dark Energy Versus Modified Gravity,” *Ann. Rev. Nucl. Part. Sci.* **66** (2016) 95–122, [arXiv:1601.06133 \[astro-ph.CO\]](#).
- [20] E. Di Valentino *et al.*, “In the realm of the Hubble tension — a review of solutions,” *Class. Quant. Grav.* **38** no. 15, (2021) 153001, [arXiv:2103.01183 \[astro-ph.CO\]](#).
- [21] L. Heisenberg, H. Villarrubia-Rojo, and J. Zosso, “Simultaneously solving the H_0 and σ_8 tensions with late dark energy,” [arXiv:2201.11623 \[astro-ph.CO\]](#).
- [22] L. Perivolaropoulos and F. Skara, “Challenges for Λ CDM: An update,” *New Astron. Rev.* **95** (2022) 101659, [arXiv:2105.05208 \[astro-ph.CO\]](#).
- [23] W. Cardona and M. A. Sabogal, “Holographic energy density, dark energy sound speed, and tensions in cosmological parameters: H_0 and S_8 ,” [arXiv:2210.13335 \[astro-ph.CO\]](#).
- [24] R.-Y. Guo, J.-F. Zhang, and X. Zhang, “Can the H_0 tension be resolved in extensions to Λ CDM cosmology?,” *JCAP* **02** (2019) 054, [arXiv:1809.02340 \[astro-ph.CO\]](#).
- [25] P. Agrawal, F.-Y. Cyr-Racine, D. Pinner, and L. Randall, “Rock ‘n’ Roll Solutions to the Hubble Tension,” [arXiv:1904.01016 \[astro-ph.CO\]](#).
- [26] L. Heisenberg and H. Villarrubia-Rojo, “Proca in the sky,” *JCAP* **03** (2021) 032, [arXiv:2010.00513 \[astro-ph.CO\]](#).
- [27] T. Clifton, P. G. Ferreira, A. Padilla, and C. Skordis, “Modified Gravity and Cosmology,” *Phys. Rept.* **513** (2012) 1–189, [arXiv:1106.2476 \[astro-ph.CO\]](#).
- [28] L. Heisenberg, R. Kase, and S. Tsujikawa, “Cosmology in scalar-vector-tensor theories,” *Phys. Rev. D* **98** no. 2, (2018) 024038, [arXiv:1805.01066 \[gr-qc\]](#).
- [29] W. Cardona, J. B. Orjuela-Quintana, and C. A. Valenzuela-Toledo, “An effective fluid description of scalar-vector-tensor theories under the sub-horizon and quasi-static approximations,” *JCAP* **08** no. 08, (2022) 059, [arXiv:2206.02895 \[astro-ph.CO\]](#).
- [30] A. Heavens *et al.*, “No evidence for extensions to the standard cosmological model,” *Phys. Rev. Lett.* **119** no. 10, (2017) 101301, [arXiv:1704.03467 \[astro-ph.CO\]](#).
- [31] S. Singh *et al.*, “On the detection of a cosmic dawn signal in the radio background,” [arXiv:2112.06778 \[astro-ph.CO\]](#).
- [32] R. Arjona, A. Melchiorri, and S. Nesseris, “Testing the Λ CDM paradigm with growth rate data and machine learning,” *JCAP* **05** no. 05, (2022) 047, [arXiv:2107.04343 \[astro-ph.CO\]](#).
- [33] **Euclid** Collaboration, D. Camarena *et al.*, “Euclid: Testing the Copernican principle with next-generation surveys,” [arXiv:2207.09995 \[astro-ph.CO\]](#).
- [34] W. Cardona, R. Arjona, A. Estrada, and S. Nesseris, “Cosmological constraints with the Effective Fluid approach for Modified Gravity,” *JCAP* **05** (2021) 064, [arXiv:2012.05282 \[astro-ph.CO\]](#).
- [35] **SDSS** Collaboration, M. Tegmark *et al.*, “The 3-D power spectrum of galaxies from the SDSS,” *Astrophys. J.* **606** (2004) 702–740, [arXiv:astro-ph/0310725](#).
- [36] **BOSS** Collaboration, S. Alam *et al.*, “The clustering of galaxies in the completed SDSS-III Baryon Oscillation Spectroscopic Survey: cosmological analysis of the DR12 galaxy sample,” *Mon. Not. Roy. Astron. Soc.* **470** no. 3, (2017) 2617–2652, [arXiv:1607.03155 \[astro-ph.CO\]](#).
- [37] S. Dodelson and F. Schmidt, *Modern Cosmology*. Elsevier Science, 2020.
- [38] D. Blas, J. Lesgourgues, and T. Tram, “The Cosmic Linear Anisotropy Solving System (CLASS). Part II: Approximation schemes,” *Journal of Cosmology and Astroparticle Physics* **2011** no. 07, 034–034.
- [39] A. Lewis, A. Challinor, and A. Lasenby, “Efficient computation of CMB anisotropies in closed FRW models,” *Astrophys. J.* **538** (2000) 473–476, [arXiv:astro-ph/9911177](#).
- [40] J. M. Bardeen, J. R. Bond, N. Kaiser, and A. S. Szalay, “The Statistics of Peaks of Gaussian Random Fields,” *Astrophys. J.* **304** (1986) 15–61.
- [41] M. S. Turner, “The Road to Precision Cosmology,” [arXiv:2201.04741 \[astro-ph.CO\]](#).
- [42] D. J. Eisenstein and W. Hu, “Baryonic features in the matter transfer function,” *Astrophys. J.* **496** (1998) 605, [arXiv:astro-ph/9709112](#).

- [43] D. Boyanovsky, H. J. de Vega, and N. G. Sanchez, “The dark matter transfer function: free streaming, particle statistics and memory of gravitational clustering,” *Phys. Rev. D* **78** (2008) 063546, [arXiv:0807.0622 \[astro-ph\]](#).
- [44] A. Dvornik *et al.*, “KiDS-1000: Combined halo-model cosmology constraints from galaxy abundance, galaxy clustering and galaxy-galaxy lensing,” [arXiv:2210.03110 \[astro-ph.CO\]](#).
- [45] N. Schöneberg, L. Verde, H. Gil-Marín, and S. Brieden, “BAO+BBN revisited – Growing the Hubble tension with a 0.7km/s/Mpc constraint,” [arXiv:2209.14330 \[astro-ph.CO\]](#).
- [46] G. Carleo *et al.*, “Machine learning and the physical sciences,” *Rev. Mod. Phys.* **91** no. 4, (2019) 045002, [arXiv:1903.10563 \[physics.comp-ph\]](#).
- [47] M. Schmidt and H. Lipson, “Distilling Free-Form Natural Laws from Experimental Data,” *Science* **324** (2009) 81–85.
- [48] S. L. Brunton, J. L. Proctor, and J. N. Kutz, “Discovering governing equations from data by sparse identification of nonlinear dynamical systems,” *Proceedings of the National Academy of Sciences* **113** no. 15, (2016) 3932–3937, [arXiv:1509.03580 \[math.DS\]](#).
- [49] D. Izzo, F. Biscani, and A. Mereta, “Differentiable Genetic Programming,” *arXiv e-prints* (2016) , [arXiv:1611.04766 \[cs.NE\]](#).
- [50] S.-M. Udrescu and M. Tegmark, “AI Feynman: a Physics-Inspired Method for Symbolic Regression,” *Sci. Adv.* **6** no. 16, (2020) eaay2631, [arXiv:1905.11481 \[physics.comp-ph\]](#).
- [51] M. Cranmer *et al.*, “Discovering Symbolic Models from Deep Learning with Inductive Biases,” [arXiv:2006.11287 \[cs.LG\]](#).
- [52] Z. Liu and M. Tegmark, “Machine Learning Hidden Symmetries,” *Phys. Rev. Lett.* **128** no. 18, (2022) 180201, [arXiv:2109.09721 \[cs.LG\]](#).
- [53] J. Koza and J. Koza, *Genetic Programming: On the Programming of Computers by Means of Natural Selection*. Bradford, 1992.
- [54] R. Arjona and S. Nesseris, “Hints of dark energy anisotropic stress using Machine Learning,” *JCAP* **11** (2020) 042, [arXiv:2001.11420 \[astro-ph.CO\]](#).
- [55] **EUCLID** Collaboration, M. Martinelli *et al.*, “Euclid: Forecast constraints on the cosmic distance duality relation with complementary external probes,” *Astron. Astrophys.* **644** (2020) A80, [arXiv:2007.16153 \[astro-ph.CO\]](#).
- [56] R. Arjona and S. Nesseris, “Novel null tests for the spatial curvature and homogeneity of the Universe and their machine learning reconstructions,” *Phys. Rev. D* **103** no. 10, (2021) 103539, [arXiv:2103.06789 \[astro-ph.CO\]](#).
- [57] **Euclid** Collaboration, M. Martinelli *et al.*, “Euclid: Constraining dark energy coupled to electromagnetism using astrophysical and laboratory data,” *Astron. Astrophys.* **654** (2021) A148, [arXiv:2105.09746 \[astro-ph.CO\]](#).
- [58] A. Aizpuru, R. Arjona, and S. Nesseris, “Machine learning improved fits of the sound horizon at the baryon drag epoch,” *Phys. Rev. D* **104** no. 4, (2021) 043521, [arXiv:2106.00428 \[astro-ph.CO\]](#).
- [59] **Euclid** Collaboration, S. Nesseris *et al.*, “Euclid: Forecast constraints on consistency tests of the Λ CDM model,” *Astron. Astrophys.* **660** (2022) A67, [arXiv:2110.11421 \[astro-ph.CO\]](#).
- [60] G. Alestas, L. Kazantzidis, and S. Nesseris, “Machine learning constraints on deviations from general relativity from the large scale structure of the Universe,” [arXiv:2209.12799 \[astro-ph.CO\]](#).
- [61] B. A. Reid. *et al.*, “Cosmological constraints from the clustering of the Sloan Digital Sky Survey DR7 luminous red galaxies,” *Mon. Not. Roy. Astron. Soc.* **404** no. 1, (2010) 60–85, [arXiv:0907.1659 \[astro-ph.CO\]](#).
- [62] A. Díaz Rivero, C. Dvorkin, F.-Y. Cyr-Racine, J. Zavala, and M. Vogelsberger, “Gravitational Lensing and the Power Spectrum of Dark Matter Substructure: Insights from the ETHOS N-body Simulations,” *Phys. Rev. D* **98** no. 10, (2018) 103517, [arXiv:1809.00004 \[astro-ph.CO\]](#).
- [63] S. Chabanier, M. Millea, and N. Palanque-Delabrouille, “Matter power spectrum: from Ly α forest to CMB scales,” *Mon. Not. Roy. Astron. Soc.* **489** no. 2, (2019) 2247–2253, [arXiv:1905.08103 \[astro-ph.CO\]](#).
- [64] J. Lesgourgues, G. Mangano, G. Miele, and S. Pastor, *Neutrino Cosmology*. Cambridge University Press, 2, 2013.
- [65] **KATRIN** Collaboration, M. Aker *et al.*, “Direct neutrino-mass measurement with sub-electronvolt sensitivity,” *Nature Phys.* **18** no. 2, (2022) 160–166, [arXiv:2105.08533 \[hep-ex\]](#).
- [66] D. J. Eisenstein and W. Hu, “Power spectra for cold dark matter and its variants,” *Astrophys. J.* **511** (1997) 5, [arXiv:astro-ph/9710252](#).
- [67] J. R. Bond and A. S. Szalay, “The collisionless damping of density fluctuations in an expanding universe,” *Astrophys. J., Lett. Ed.* **274** (1983) 443–468.
- [68] J. R. Bond and G. Efsthathiou, “Cosmic background radiation anisotropies in universes dominated by nonbaryonic dark matter,” *Astrophys. J., Lett. Ed.* **285** (1984) L45–L48.
- [69] E. W. Kolb and M. S. Turner, *The Early Universe*, vol. 69. Front. Phys., 1990.
- [70] B. C. Allanach, D. Grellscheid, and F. Quevedo, “Genetic algorithms and experimental discrimination of SUSY models,” *JHEP* **07** (2004) 069, [arXiv:hep-ph/0406277](#).
- [71] Y. Akrami, P. Scott, J. Edsjo, J. Conrad, and L. Bergstrom, “A Profile Likelihood Analysis of the Constrained MSSM with Genetic Algorithms,” *JHEP* **04** (2010) 057, [arXiv:0910.3950 \[hep-ph\]](#).
- [72] S. Abel, D. G. Cerdeño, and S. Robles, “The Power of Genetic Algorithms: what remains of the pMSSM?,” [arXiv:1805.03615 \[hep-ph\]](#).
- [73] X.-L. Luo, J. Feng, and H.-H. Zhang, “A genetic algorithm for astroparticle physics studies,” *Comput. Phys. Commun.* **250** (2020) 106818,

- [arXiv:1907.01090 \[astro-ph.HE\]](#).
- [74] M. Ho *et al.*, “A Robust and Efficient Deep Learning Method for Dynamical Mass Measurements of Galaxy Clusters,” *Astrophys. J.* **887** (2019) 25, [arXiv:1902.05950 \[astro-ph.CO\]](#).
 - [75] C. Bogdanos and S. Nesseris, “Genetic Algorithms and Supernovae Type Ia Analysis,” *JCAP* **05** (2009) 006, [arXiv:0903.2805 \[astro-ph.CO\]](#).
 - [76] S. Nesseris and A. Shafieloo, “A model independent null test on the cosmological constant,” *Mon. Not. Roy. Astron. Soc.* **408** (2010) 1879–1885, [arXiv:1004.0960 \[astro-ph.CO\]](#).
 - [77] S. Nesseris and J. García-Bellido, “A new perspective on Dark Energy modeling via Genetic Algorithms,” *JCAP* **11** (2012) 033, [arXiv:1205.0364 \[astro-ph.CO\]](#).
 - [78] S. Nesseris and J. García-Bellido, “Comparative analysis of model-independent methods for exploring the nature of dark energy,” *Phys. Rev. D* **88** no. 6, (2013) 063521, [arXiv:1306.4885 \[astro-ph.CO\]](#).
 - [79] D. Sapone, E. Majerotto, and S. Nesseris, “Curvature versus distances: Testing the FLRW cosmology,” *Phys. Rev. D* **90** no. 2, (2014) 023012, [arXiv:1402.2236 \[astro-ph.CO\]](#).
 - [80] R. Arjona and S. Nesseris, “What can Machine Learning tell us about the background expansion of the Universe?,” *Phys. Rev. D* **101** no. 12, (2020) 123525, [arXiv:1910.01529 \[astro-ph.CO\]](#).
 - [81] **VIRGO Consortium** Collaboration, R. E. Smith, J. A. Peacock, A. Jenkins, S. D. M. White, C. S. Frenk, F. R. Pearce, P. A. Thomas, G. Efstathiou, and H. M. P. Couchmann, “Stable clustering, the halo model and nonlinear cosmological power spectra,” *Mon. Not. Roy. Astron. Soc.* **341** (2003) 1311, [arXiv:astro-ph/0207664](#).
 - [82] F. Renzi, N. B. Hogg, M. Martinelli, and S. Nesseris, “Strongly lensed supernovae as a self-sufficient probe of the distance duality relation,” *Phys. Dark Univ.* **32** (2021) 100824, [arXiv:2010.04155 \[astro-ph.CO\]](#).
 - [83] R. Arjona, H.-N. Lin, S. Nesseris, and L. Tang, “Machine learning forecasts of the cosmic distance duality relation with strongly lensed gravitational wave events,” *Phys. Rev. D* **103** no. 10, (2021) 103513, [arXiv:2011.02718 \[astro-ph.CO\]](#).